

Electron Spin Resonance and Optical Spectra of V^{2+} in $NaCl$ †

GORO KUWABARA*

Argonne National Laboratory, Argonne, Illinois

(Received 12 October 1964)

The ESR and optical spectra of V^{2+} in $NaCl$ show that there are two species of V^{2+} , one of which is situated in a tetragonal and another in an orthorhombic site. Optically, three weak bands corresponding to transitions between Stark levels and one strong electron-transfer band were detected which yield the crystal field strength $\Delta = 8190 \text{ cm}^{-1}$ and the Racah parameter $B = 559 \text{ cm}^{-1}$. Two long-wavelength bands show some structure which is probably due to splitting by low-symmetry fields. The g shift and zero-field splitting of the center in the tetragonal site suggest that the d orbitals are considerably distorted by covalency.

INTRODUCTION

RECENTLY, a great deal of experimental work on the optical spectra of transition metal ions in crystals has been reported and analyzed successfully with crystal field theory. The parameters introduced thereby have complicated origins so that in order to obtain a better understanding of the electronic states of impurities in solids, it is desirable to study the variation of these parameters for the same ion in different crystals. However, most of the previous work has been confined to trivalent and divalent crystals such as Al_2O_3 , MgO , and ZnS which have a fair amount of covalency. As far as we know, no work has been reported on the alkali halides which have the simplest bonding character.

This investigation was undertaken with two purposes in mind. The first of these was to determine the crystal field parameters of a transition metal ion in an alkali-halide lattice while the second was to study further the effects of environment, especially an ion vacancy, on the optical spectra of impurities in solids; Schawlow¹ has already reported the splitting of the 2E level of Cr^{3+} in MgO . For this second purpose, it is preferable to work on a system in which the point symmetry around the impurity ion is precisely determined by spin resonance techniques, and the electronic state in the crystal can be easily correlated with that of the free ion and is still sensitive to the surroundings. Furthermore, it is desirable that the association of a vacancy with an impurity ion be controlled intentionally. Divalent metal ions incorporated into alkali halides are presumed to go into substitutional or interstitial sites. If charge compensation occurs through the inclusion of positive ion vacancies which are associated with the divalent ions, the impurity ions will be acted on by weak fields of low symmetry such as tetragonal or orthorhombic. These fields are superposed on the strong fields of octahedral or tetrahedral symmetry from surrounding halogen ions.

Favorable conditions for divalent ions are that they have Kramer's degeneracy, an orbitally nondegenerate

ground state, and a half-filled shell configuration in the strong field scheme. Because of these facts we can easily obtain the spin-resonance signal, and also can expect sharp absorption or emission lines² as well as fairly strong broad bands in optical spectra. Divalent ions with d^3 configuration in octahedral sites or those with d^7 configuration in tetrahedral sites are desirable.

The ESR of Mn^{2+} in alkali halides was extensively studied by Watkins³ and Itoh.⁴ However, in the case of ions with a d^5 configuration in an octahedral site, all optical transitions between Stark levels are doubly forbidden so that we cannot expect to detect optical absorption bands with crystals containing a reasonable concentration of impurity.

Because of the above reasons, $NaCl$ was chosen as a host crystal and V^{2+} as an impurity ion; moreover, the spin resonance as well as the optical spectra⁵ of V^{2+} in⁶ Al_2O_3 and⁷ MgO have already been reported.

PREPARATION OF SAMPLES

Anhydrous vanadium dichloride was obtained by placing pure vanadium metal in a quartz tube, heating it in a stream of hydrogen chloride, and collecting the rather pure greenish flakes which grew on the cool part of the tube wall.

$NaCl$ crystals were grown by the Bridgeman method in vacuum or helium atmosphere. Considerable precautions are necessary because the divalent vanadium is easily oxidized. In order to avoid oxidation the following procedure was used⁸:

Two quartz ampoules were connected in series. The lower ampoule had a conical bottom and was used as the container for the growth of the single crystal. The top ampoule contained a fine quartz filter, above which was placed a piece of vanadium metal and pure single crystals of $NaCl$. A side arm containing VCl_2 was also sealed to the top ampoule above the quartz filter. After the system was evacuated for at least 2 h the $NaCl$

² S. Sugano, *Progr. Theoret. Phys. (Kyoto)*, Suppl. **14**, 66 (1960).

³ G. Watkins, *Phys. Rev.* **113**, 79 (1959).

⁴ J. Itoh, *J. Phys. Soc. Japan* **13**, 1174 (1958).

⁵ M. Sturge, *Phys. Rev.* **130**, 639 (1963).

⁶ J. Lambe and C. Kikuchi, *Phys. Rev.* **118**, 71 (1960).

⁷ W. Low, *Phys. Rev.* **101**, 1827 (1956).

⁸ This procedure was suggested by Dr. D. Gruen.

† Based on work performed under the auspices of the U. S. Atomic Energy Commission.

* On leave of absence from the University of Tokyo, Tokyo, Japan.

¹ A. L. Schawlow, *J. Appl. Phys.* **33**, 395 (1962).

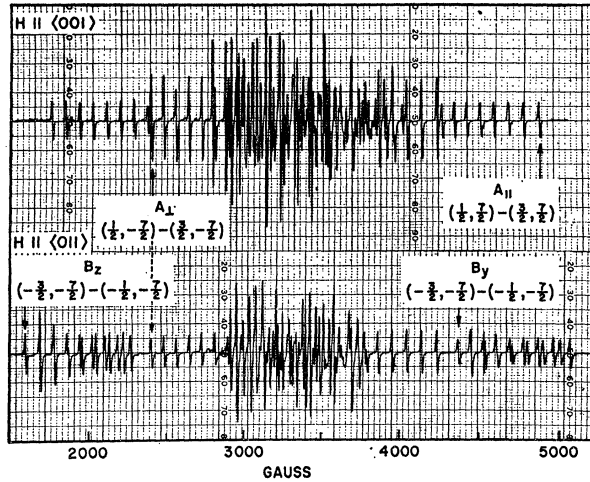


FIG. 1. Spin resonance of V^{2+} in NaCl at room temperature.

was melted and the VCl_2 (from 0.05 to 0.5% by weight) was dropped from the side arm into the melted salt. Helium pressure was then applied forcing the molten salt with the dissolved VCl_2 into the bottom ampoule. The bottom ampoule was then sealed off and transferred to the growing furnace. The single crystals obtained in this manner were annealed in the tube used for growing. Crystals containing a high concentration of V^{2+} are colored a light pink. The concentration of V^{2+} in the grown crystals was obtained by chemical analysis.

THE ELECTRON-SPIN-RESONANCE SPECTRA

The spin-resonance spectra were obtained with a Varian spectrometer operating in the X-band region at room and liquid nitrogen temperatures, and were studied by rotating a crystal (ca. $2 \times 2 \times 3$ mm) around a cube edge or a face diagonal. The spectra at room temperature for $H \parallel [001]$ and $H \parallel [011]$ are shown in Fig. 1. About 100 strong lines are observed between 1500 and 5000 G. In the favorable directions of magnetic field, the linewidth is about 8 G. Almost all lines can be grouped into sets of eight lines. In most orientations of the magnetic field, many lines overlap in the central part of the spectrum. By observing the behavior under rotation, these lines are classified into two groups, one of which is due to a center of tetragonal symmetry with axes in cube edge directions (A type), and another is due to a center of low symmetry with axes in $z = [011]$, $y = [0\bar{1}1]$ and $x = [100]$ directions (B type). Eight lines which constitute a set come from nuclear hyperfine structure due to V^{51} (99.8%) $I = \frac{7}{2}$.

The ground state of V^{2+} is 4A_2 in octahedral surroundings. To analyze the spectra, the following spin Hamiltonian was used:

$$\begin{aligned} \mathcal{H}/h\nu_0 = & g_x S_z H_x + g_y S_y H_y + D[S_z^2 - S(S+1)/3] \\ & + E(S_x^2 - S_y^2) + A I_z S_z + B I_x S_x + C I_y S_y, \\ & S = \frac{3}{2}, \quad I = \frac{7}{2}. \end{aligned}$$

The distortion axes were chosen as Z axes in both cases. The coefficients of the spin Hamiltonian, which give the least-squares fit were determined by solving the secular equation with a computer⁹ starting from the approximate values obtained by a perturbation method because the zero field splittings are fairly large in both cases. These values are listed in Table I. The relative signs of D , E , and A were determined from the change in hyperfine splitting associated with electronic transitions and turned out to be the same. The absolute sign cannot be determined definitely without experiments at low temperature. However, as will be discussed in a later section, D is thought to be negative in the A -type center and might also be negative in the B -type center since the absolute values of the hyperfine constants are nearly the same for A - and B -type centers.

From symmetry considerations, we expect three sets of spectra due to A -type centers and six sets of spectra due to B -type centers for an arbitrary direction of magnetic field. For special directions, some of them coincide. However, the spectra due to the centers whose distortion axes make angles other than 0 or 90 deg with the magnetic field were difficult to identify. This is mainly due to the broadening of $(\pm \frac{3}{2} \leftrightarrow \pm \frac{1}{2})$ lines and the overlapping of many spectra in the central part when the magnetic field is applied to directions other than a cube edge or a face diagonal. For example, when the magnetic field is applied at an angle of 60 or 45 deg to the Z axis or parallel to the X axis of the B -type center, lines corresponding to $(\pm \frac{3}{2} \leftrightarrow \pm \frac{1}{2})$ transitions also appear in the central part and overlap with other $(\frac{1}{2} \leftrightarrow -\frac{1}{2})$ transition lines.

The doped NaCl crystals, especially of high impurity concentration, showed irregularities on the cleaved surfaces probably indicating strains and faults in growth. These irregularities cause changes in the crystal field parameters D and E and also variations in orientation of the distortion axis from site to site and thus probably account for the broadening of the $(\pm \frac{3}{2} \leftrightarrow \pm \frac{1}{2})$ lines when the magnetic field is applied in a direction other than along a symmetry axis. When

TABLE I. Constants of spin Hamiltonians of V^{2+} in NaCl.

Symmetry	A-type center		B-type center	
	Tetragonal		Orthorhombic	
Axes	[100], [010], [001]		$x[100]$, $y[0\bar{1}1]$, $z[011]$	
g	$g_{11} = 1.9704 \pm 0.0006$ $g_{12} = 1.9754 \pm 0.0006$		$g_x = 1.969 \pm 0.001$ $g_y = 1.970 \pm 0.001$ $g_z = 1.976 \pm 0.001$	
$D (10^{-4} \text{ cm}^{-1})$	(-) 572.4 ± 0.7		(-) 655 ± 1	
$E (10^{-4} \text{ cm}^{-1})$	(+) 0.5 ± 0.7		(-) 197 ± 1	
$A (10^{-4} \text{ cm}^{-1})$	$A = (-) 80.5 \pm 0.7$ $B = (-) 78.8 \pm 0.7$		$A = (-) 81 \pm 1$ $B = (-) 80 \pm 1$ $C = (-) 81 \pm 1$	

⁹ The program was developed by Dr. J. Gabriel. See J. W. Wilkens and J. R. Gabriel, Phys. Rev. **132**, 1950 (1963).

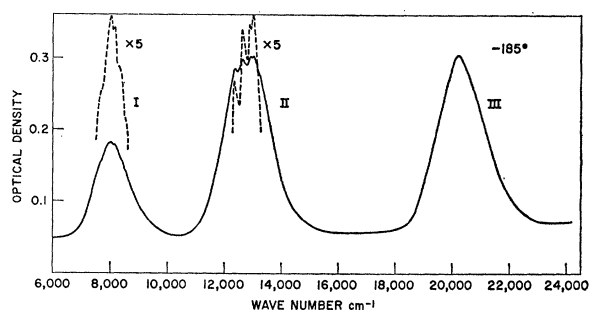


FIG. 2. Optical absorption spectra of V^{2+} at 77°K .

a crystal is quenched rapidly from 500°C by dropping it on a metal plate, the above-mentioned lines almost disappear even for a magnetic field along the face diagonal because of the strains induced by rapid cooling. The line pattern is returned to its normal state after the quenched crystal is annealed.

Vanadium has four valency states. The iron group ions with higher valency than three are unlikely to exist in alkali halides as an atomically dispersed state because of difference in ionic radius and difficulty in charge compensation. Further, if we take into consideration the fact that the spin-resonance signal can hardly be detected at room temperature for ions with orbitally degenerate ground states, we can exclude the possibility of V^+ and V^{3+} in substitutional (cubic) and V^{2+} in interstitial (tetrahedral) sites as the centers. The only possible species other than V^{2+} is vanadyl ion VO^{2+} . However, VO^{2+} has one d electron ($S=\frac{1}{2}$) and therefore a fast spin-lattice relaxation time. Also, it has only one absorption band in the optical spectrum. Therefore, it is concluded that the centers we are dealing with are V^{2+} ions in distorted octahedral sites.

The intensity ratio of the signals due to the two types of centers are nearly the same and almost independent of the concentration or heat treatment.

No isotropic spectrum due to V^{2+} in a cubic site has been identified so far. The ratio of numbers of the two centers is almost independent of heat treatment or concentration so that it may be concluded that the V^{2+} ions incorporated into the NaCl lattice substitute for Na^+ ions and are always accompanied by positive ion vacancies in either the nearest (B -type center) or next nearest (A -type center) cation site and that these entities are fairly stable. No change of spectrum with time due to aggregation of impurities could be observed which is quite different from the behavior of Mn^{2+} in alkali halides. There seems to be little possibility that the A -type center is due to V^{2+} associated with negative divalent impurities.

In addition to the lines described above, numerous weak lines whose intensities are mostly less than one-tenth of those of the main lines were observed in the low-field region down to around 500 G. Some of these can be grouped into sets of eight lines, and their intensity ratios to the main lines vary with concentra-

tion. These spectra were not studied, but it is thought that some of them may be due to ion pairs and some to forbidden transitions. The calculation shows that the transition probabilities of the forbidden lines are around a few percent of those of the allowed transitions. On cooling to -185°C , slight changes of D and E took place; otherwise the spectra were unchanged. No saturation effects were observed.

OPTICAL SPECTRA

Optical absorption spectra between 200 and $2500\text{ m}\mu$ were studied with a Cary Model 14 R spectrophotometer and are shown in Fig. 2. At 77°K , three weak bands and one strong one have been observed and are located at 8190, 12 800, 20 250 and $42\,300\text{ cm}^{-1}$; these are designated bands I, II, III, and IV, respectively. They are listed in Table II, together with the approximate values of the oscillator strengths. On warming to room temperature, the bands shift a little bit towards lower energy and become broader, the intensities increase by about 40%, and the structure disappears in bands I and II. Below 77°K down to liquid-helium temperature, shapes and intensities remain almost constant.

The low values of the oscillator strengths and their temperature dependence suggests that bands I, II, and III correspond to transitions between Stark levels of d^3 configurations. Band IV, which is stronger than the other bands by a factor of 70, is assigned to a charge transfer band.

The ground state of $V^{2+}(3d^3)$ is ${}^4A_2(t_2^3)$. Other quartet states of the d^3 configuration are ${}^4T_2(t_2^2e)$, ${}^4T_1(a)$ and ${}^4T_1(b)$ in order of increasing energies. It is thus possible to assign the three weak bands to intra-system transitions from 4A_2 to these three quartet states almost uniquely.

TABLE II. Absorption bands of V^{2+} in NaCl.^a

Band	Observed (cm^{-1})	Calculated (cm^{-1})	Oscillator strength	Transition ${}^4A_2(t_2^3) \rightarrow$
IV	42 300		4.4×10^{-2}	
III	20 250	20 140 (15 800)	6.0×10^{-4}	${}^4T_1(b)$ ${}^2T_2(t_2^3)$
II	12 800 13 070 12 950 12 650 12 400	12 740 (10 500)	6.0×10^{-4}	${}^4T_1(a)$ ${}^2T_1(t_2^3)$ ${}^2E(t_2^3)$
I	8190 8550 8400 8230 8050 7650	8190	2.4×10^{-4}	${}^4T_2(t_2^2e)$]

^a $Dq=819\text{ cm}^{-1}$, $C=4.3B$, $B=559\text{ cm}^{-1}$.

TABLE III. Crystal field and racah parameters of V^{2+} and Ni^{2+} in various crystals.

Ion	Host crystal	Cation-anion distance of host crystal			Ref.
		(A)	Dq (cm^{-1})	B (cm^{-1})	
V^{2+}	aqueous		1260	460	755
V^{2+}	MgO	2.10	1320	550	5
V^{2+}	Al_2O_3	1.89			
		1.93	1360	550	5
V^{2+}	NaCl	2.81	819	559	this paper
Ni^{2+}	aqueous		850	887	1050
Ni^{2+}	MgO	2.10	860	866	11
Ni^{2+}	NaCl	2.81	678	800	12

Using the energy matrices of Tanabe and Sugano¹⁰ we get $Dq=819\text{ cm}^{-1}$ and $B=559\text{ cm}^{-1}$. $\Delta=10Dq$ is the intensity of the cubic field and B is the parameter associated with the Coulomb interaction energy introduced by Racah. B is smaller than the free ion value $B_0=766\text{ cm}^{-1}$ by about 27%.

In Table III^{11,12} some of the previous results on single crystals are listed for comparison. It will be noticed that Dq values are fairly small in NaCl, while B values are nearly the same as those in other crystals. The crystal field strength in NaCl is, however, very much larger than the values expected from the simple point ion model.

In addition to the quartet states, there are several doublet states from which we can expect weak but rather sharp line spectra corresponding to transitions from the ground to the doublet states belonging to the t_2^3 configuration. The calculated positions of line spectra listed in Table II were estimated by assuming the relation $C=4.3B$ between two Racah parameters. No line spectra have been detected as yet, probably because of the weak intensity of the transitions and limited resolution of the spectrophotometer. The isoelectronic ion Cr^{3+} , analogous to V^{2+} , shows a characteristic red luminescence in Al_2O_3 and MgO. However, in NaCl: V^{2+} no luminescence was detected by excitation with light in band II. This fact is not surprising because in this case, due to the small value of Dq , the 2E level lies above the 4T_2 level contrary to the case of ruby, so that the excited ion may return to the ground state nonradiatively through the 4T_2 state. The wave functions of $^4T_1(a)$ and $^4T_1(b)$ are

$$\Psi_a(^4T_1) = -\sin\theta\Psi_1(^4T_1(t_2^2e)) + \cos\theta\Psi_2(^4T_1(t_2e^2)), \quad (1)$$

$$\Psi_b(^4T_1) = \cos\theta\Psi_1(^4T_1(t_2^2e)) + \sin\theta\Psi_2(^4T_1(t_2e^2)), \quad (2)$$

$$\tan 2\theta = -12B/(10Dq - 9B). \quad (3)$$

For the purpose of calculating the intensities of the $^4A_2 \rightarrow ^4T_1(a)$ and $^4A_2 \rightarrow ^4T_1(b)$ transitions, the $^4T_1(t_2e^2)$ part of the wave function may be ignored since the

transition to the $^4T_1(t_2e^2)$ part is a two-electron excitation and the matrix element should be small. Therefore, the ratio of the intensities of the two corresponding transitions, i.e., bands II and III, is simply the square of the ratio of the coefficients $-\sin\theta$ and $\cos\theta$ from Eqs. (1) and (2).

$$I_{(II)}/I_{(III)} = \nu_{II}/\nu_{III} \tan^2\theta, \quad (4)$$

where I_{II} and I_{III} are the intensities of bands II and III, respectively.

$\tan\theta$ may be determined by substituting the known values of B and Dq in Eq. (3) and gives $I_{(II)}/I_{(III)}=1.6$. The experimentally measured intensity ratio is 1.0. The discrepancy might be ascribed to the difference in mixing of odd states into excited states because the $^4T_1(b)$ state lies higher than the $^4T_1(a)$ state.

If the hemihedral potentials, which allow the transitions, come from odd vibrations, the absorption intensities are expected to be constant at low temperatures and increase linearly with temperature above the Debye temperature (320°K for NaCl). On the other hand, if the potential is mainly due to asymmetry of surrounding ions, the intensities are expected to be insensitive to temperature. Although the temperature range studied was not wide enough, the result seems to indicate that the selection rules are relaxed by thermal vibrations above liquid-nitrogen temperature.

SPLITTING OF EXCITED STATES

Since there is little possibility of overlapping of line spectra with the band spectra as seen in Table II, the observed structure in bands I and II may be attributed to vibration and/or to the splittings of electronic levels by lower symmetry fields and spin-orbit interaction.

The parameters of the low-symmetry field and spin-orbit interaction are usually determined by comparing calculated and observed splittings. However, in the present case the electron-spin-resonance data show that two kinds of V^{2+} with different symmetries exist in nearly equal amounts. Their ratio could not be controlled so that it is difficult to separate the two kinds of spectra which overlap each other. Therefore, we have to be content with qualitative discussion and only the splitting of excited states by lower symmetry fields,

TABLE IV. A -type center.^a

D_4	Splittings
$^4T_2(t_2^2e) \left\{ \begin{array}{l} 0 \ ^4B_2 \\ \pm 1 \ ^4E \end{array} \right.$	$-2[(v/3) - (v'/4)]$ $(v/3) - (v'/4)$
$^4T_1(t_2^2e) \left\{ \begin{array}{l} 0 \ ^4A_2 \\ \pm 1 \ ^4E \end{array} \right.$	$-2[(v/3) + (v'/4)]$ $(v/3) + (v'/4)$
$^4T_1(t_2e^2) \left\{ \begin{array}{l} 0 \ ^4A_2 \\ \pm 1 \ ^4E \end{array} \right.$	$2v/3$ $-v/3$

^a The quantities v and v' are defined by Eq. (7).

¹⁰ Y. Tanabe and S. Sugano, J. Phys. Soc. Japan 9, 753 (1954).

¹¹ W. Low, Phys. Rev. 109, 247 (1958).

¹² M. Nasu, thesis, University of Tokyo, 1963 (unpublished).

TABLE V. B -type center.^a

D_2	Splittings
${}^4T_2(t_2^2e)$ $\begin{cases} {}^4A \\ {}^4B_1 \\ {}^4B_2 \end{cases}$	$\begin{cases} -2[(v/3) - (v'/4)] \\ (v/3) - (v'/4) - (t/4) \\ (v/3) - (v'/4) + (t/4) \end{cases}$
${}^4T_1(t_2^2e)$ $\begin{cases} {}^4B_3 \\ {}^4B_2 \\ {}^4B_1 \end{cases}$	$\begin{cases} -2[(v/3) + (v'/4)] \\ (v/3) + (v'/4) - (t/4) \\ (v/3) + (v'/4) + (t/4) \end{cases}$
${}^4T_1(t_2e^2)$ $\begin{cases} {}^4B_3 \\ {}^4B_2 \\ {}^4B_1 \end{cases}$	$\begin{cases} 2v/3 \\ -(v/3) - (t/2) \\ -(v/3) + (t/3) \end{cases}$

^a The quantities v , v' , and t are defined by Eq. (9).

which are correlated with the constants in the spin-Hamiltonian, will be considered.

The quadratic noncubic potentials caused by the positive ion vacancy at the next nearest (A -type) or nearest (B -type) cation site are written as

$$V_A = E_u V_u(E) + f(r^2), \quad (5)$$

$$V_B = E_A V_A(E) + T_{2,A} V_A(T_2) + f'(r^2), \quad (6)$$

where $V_u(E) = (5/8)^{1/2}(3z^2 - r^2)$ (axes, $x = [100]$, $y = [010]$, $z = [001]$). For computation of the B -type center, the cubic bases were transformed to span the irreducible representations of the orthorhombic (axes, $z = [011]$, $y = [0\bar{1}1]$, $x = [100]$) as well as the cubic group by the following unitary transformation:

E	$V_A(E)$	$V_{B_3}(E)$	
u	$-\frac{1}{2}$	$\sqrt{3}/2$	
v	$\sqrt{3}/2$	$\frac{1}{2}$	
T_2	$V_A(T_2)$	$V_{B_1}(T_2)$	$V_{B_2}(T_2)$
ξ	1	0	0
η	0	$1/\sqrt{2}$	$1/\sqrt{2}$
ζ	0	$1/\sqrt{2}$	$-1/\sqrt{2}$

where

$$\begin{aligned} V_A(E) &= (5/8)^{1/2}(3x^2 - r^2), & V_A(T_2) &= (15/8)^{1/2}(y^2 - z^2), \\ V_{B_3}(E) &= 30^{1/2}yz, & V_{B_1}(T_2) &= (15/2)^{1/2}xy, \\ & & V_{B_2}(T_2) &= (15/2)^{1/2}zx, \end{aligned}$$

in the case of pure d orbitals.

E_u , E_A and $T_{2,A}$ are coefficients which involve displacements and polarization of surrounding ions. The magnitudes of these coefficients are quite sensitive to the positions of ions so that we will leave them as unknown constants.

Neglecting configuration interaction, the splittings of each state referred to the original position are calculated for A - and B -type centers in Tables IV and V, respectively.

The parameters in Table IV are defined as

$$\begin{aligned} v &= -3(t_{2,\pm 1} | E_u V_u(E) | t_{2,\pm 1}) \\ &= (3/2)(t_{2,0} | E_u V_u(E) | t_{2,0}), \quad (7) \end{aligned}$$

$$v' = -2(e_u | E_u V_u(E) | e_u) = 2(e_v | E_u V_u(E) | e_v).$$

v and v' are splittings of one of each of the t_2 and e electronic levels by the tetragonal field. The signs are chosen as positive when $t_{2,\pm 1}$ and e_u states are lower.

By using (2), (3) and $({}^4T_1(t_2^2e) | V_u(E) | {}^4T_1(t_2e^2)) = 0$, the splittings of the ${}^4T_1(a)$ and ${}^4T_1(b)$ states are calculated as

D_4	Splittings
${}^4T_1(a)$ $\begin{cases} 0 \text{ } {}^4A_2 \\ \pm 1 \text{ } {}^4E \end{cases}$	$\begin{cases} (2v/3) \cos 2\theta - (v'/2) \sin^2 \theta \\ -(v/3) \cos 2\theta + (v'/4) \sin^2 \theta \end{cases}$ (8)
${}^4T_1(b)$ $\begin{cases} 0 \text{ } {}^4A_2 \\ \pm 1 \text{ } {}^4E \end{cases}$	$\begin{cases} -(2v/3) \cos 2\theta - (v'/3) \cos^2 \theta \\ (v/3) \cos 2\theta + (v'/4) \cos^2 \theta \end{cases}$

If we use pure d orbitals for t_2 and e , we obtain $v' = (4/3)v$ and the over-all splittings of 4T_2 , ${}^4T_1(a)$ and ${}^4T_1(b)$ become 0, $0.98v$ and $0.21v$, respectively.

Experimentally, similar structures were observed in bands I and II while no structure could be detected in band III. The reason for this is not clear. However, if we assume the over-all splitting of ${}^4T_1(b)$ to be zero, we obtain the relation $v' = 2.5v$ instead of $v' = 1.33v$, $0.9v$ and $1.46v$ as the splittings of 4T_2 and ${}^4T_1(a)$. This is not unreasonable because, as will be discussed in the next section, d orbitals appear to be fairly distorted in the crystal.

The parameters in Table V are defined as

$$\begin{aligned} v &= -3(t_{2,B_1} | E_A V_A(E) | t_{2,B_1}), \\ v' &= -2(e_A | E_A V_A(E) | e_A), \quad (9) \\ t &= -2(t_{2,B_1} | T_{2,A} V_A(T_2) | t_{2,B_1}). \end{aligned}$$

v , v' and t are the splittings of t_2 and e electrons by E_A and $t_{2,A}$ fields, respectively.

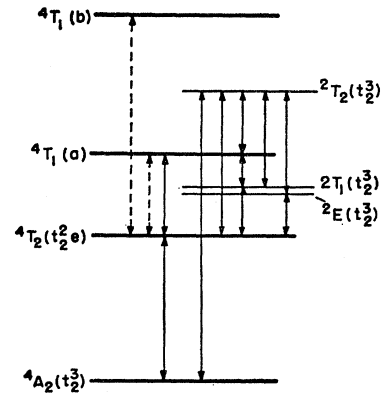


FIG. 3. Coupling scheme of d^3 system in tetragonal field. Solid line: Interaction through spin-orbit coupling. Broken line: Interaction through tetragonal field.

DISCUSSION

In this section we will consider the relation between ESR and optical spectra. For simplicity we will mainly treat the *A*-type center.

Figure 3 shows the coupling scheme of the d^3 system between states with t_2^3 and t_2^2e configurations including ${}^4T_1(t_2e^2)$ in a tetragonal field.

In the second-order calculations within this scheme the g shift (the departure of the g value from the spin-only value of 2.0023) comes from the mixing of the orbital angular momentum of the 4T_2 state by spin-orbit coupling, while the zero-field splitting $2D$ is caused by mixing of the ${}^4T_2(t_2^2e)$ and ${}^2T_2(t_2^3)$ states into the ground state by the combined action of the spin-orbit interaction and tetragonal crystal field. They are given by

$$\Delta g = 2.0023 - g, \quad \Delta g_{11} = 8\lambda_{11}'k_{11}'/E_{11}, \quad \Delta g_{\perp} = 8\lambda_{\perp}'k_{\perp}'/E_{\perp}, \quad (10)$$

$$D = 4(\lambda_{\perp}'^2/E_{\perp} - \lambda_{11}'^2/E_{11}) + 3(\lambda_{11}'^2/E_{11}' - \lambda_{\perp}'^2/E_{\perp}'), \quad (11)$$

where $\lambda_{11,i}'$ and $\lambda_{\perp,i}$ are the effective spin-orbit coupling constants in the crystal, $k_{11,i}'$ are the reduction factors of orbital angular momentum, and E_{\perp} , E_{11} , E_{\perp}' , and E_{11}' are the energies of the components of the ${}^4T_2(t_2^2e)$ and the ${}^2T_2(t_2^3)$ states from the ground state, respectively. The effects of configuration mixing and deformation of orbitals are taken into account by introducing anisotropies in λ' and k' . $E_{11} - E_{\perp} = -3(v/3 - v'/4)$, $E_{11} \cong E_{\perp} \cong \Delta \cong 8190 \text{ cm}^{-1}$, $E_{\perp} \cong E_{11} \cong 15800 \text{ cm}^{-1}$ (estimated).

If we neglect the anisotropy of λ' and the 2T_2 state, Eqs. (10) and (11) are reduced to

$$\Delta g_{11} = 8\lambda'/E_{11}, \quad \Delta g_{\perp} = 8\lambda'/E_{\perp}, \quad (12)$$

$$D = 4\lambda'^2(1/E_{\perp} - 1/E_{11}) = \lambda'/2(\Delta g_{\perp} - \Delta g_{11}). \quad (13)$$

The corresponding formulas for the *B*-type center are

$$\Delta g_x = 8\lambda'/E_A, \quad \Delta g_y = 8\lambda'/E_{B_1}, \quad \Delta g_z = 8\lambda'/E_{B_2}, \quad (14)$$

$$D = 2\lambda'^2(1/E_{A_1} + 1/E_{B_1} - 2/E_{B_2}) = \lambda'/4(\Delta g_x + \Delta g_y - 2\Delta g_z), \quad (15)$$

$$E = 2\lambda'^2(1/E_{B_1} - 1/E_{A_1}) = \lambda'/4(\Delta g_y - \Delta g_x). \quad (16)$$

In the first step, neglecting the anisotropy in g shift and putting $k'=1$, we get $\lambda'=31 \text{ cm}^{-1}$ from (12). This calculated value is reduced by about 40% from the free ion value.

The zero-field splitting $2D$ consisting of two terms is fairly complicated. Although we have no experimental information concerning the 2T_2 state, the splitting of this state is expected to be less than 1000 cm^{-1} because experimentally the over-all splittings of three quartet states corresponding to Eq. (8) were found to be less than 900 cm^{-1} , and the ${}^2T_2(t_2^3)$ state does not split in the first-order calculation.

If we assume λ' to be isotropic and $\lambda=\lambda'$, $k'=1$, the contribution of the first term to D is $\lambda'/2(\Delta g_{\perp} - \Delta g_{11}) = -0.075 \text{ cm}^{-1}$ and the absolute value of the second term is 0.012 cm^{-1} for $|E_{\perp}' - E_{11}'| = 1000 \text{ cm}^{-1}$ so that the sign of D might be determined by the first term.

If we use the simple Eqs. (12) and (13), the observed values of g , D and $10Dg = \Delta$ are consistent with each other for $E_{11} - E_{\perp} = -1000 \text{ cm}^{-1}$. Thus, the experimental values appear to be reasonable as long as we leave the splitting of the 4T_2 level as an adjustable parameter.

However, if we take pure d orbitals as t_2 and e , the 4T_2 state does not split in the first order. By mixing the ${}^4T_1(t_2^2e)$ state into the ${}^4T_2(t_2^2e)$ state through the tetragonal crystal field, the orbital doublet level 4E goes down below 4B_2 . This result contradicts the experimental one ($\Delta g_{11} > \Delta g_{\perp}$) even qualitatively so that we have to attribute the anisotropy in g shift to the anisotropy of $\lambda'k'$. Under the assumptions that $\lambda_{11}' = \lambda_{\perp}$, $\lambda_{11}' = \lambda_{\perp}$, $k_{11}'/k_{\perp}' = \lambda_{\perp}'/\lambda_{11}'$, the contribution of the first term and the absolute value of the second term of D are -0.11 cm^{-1} and 0.025 cm^{-1} for $|E_{\perp}' - E_{11}'| = 1000 \text{ cm}^{-1}$, respectively, so that also in this case the sign of D might be the same as that of the first term. We cannot decide whether the anisotropy in g shift comes from the splitting of the 4T_2 state or the anisotropy in λ' . In either case, however, we might be led to the conclusion that d orbitals are considerably distorted by covalent bonding with surrounding Cl^- ions for the following reasons. If the former is the case, the splitting of 4T_2 , which is large enough to cause the observed anisotropy in g shift, should come from distortion of orbitals, since for pure d orbitals a second-order term in the potential of the tetragonal field has no effect on the 4T_2 state in the first-order calculation, and fourth-order terms have T_1 symmetry so that their effects are small.

On the other hand, if we attribute the anisotropy in g shift to the anisotropy in λ' , about 5% of the anisotropy is needed to account for the observed value. Recently, Kamimura¹³ has explained the anisotropy of g and D for d^3 and d^8 systems in a trigonal field by taking into account the effects of covalency as well as configuration mixing. In the tetragonal case the ${}^4T_1(t_2^2e)$ state does not couple directly with the ground state and the effects of configuration mixing occur through the 4T_2 state. The mixing of ${}^4T_{1,\pm 1}(t_2^2e)$ into ${}^4T_{2,\pm 1}(t_2^2e)$ is about 10% and the anisotropy in λ' due to this mixing is only 1%, so that the rest of the anisotropy probably comes from covalency.

We will not discuss the *B*-type center because there are too many undetermined parameters. However, it is to be noted that the constants of its spin Hamiltonian in which the 4T_2 state splits in first order are nearly the same as those of the *A*-type center, so that the g shift

¹³ H. Kamimura, Phys. Rev. **128**, 1077 (1962).

and D are probably caused by the same effect for both centers.

CONCLUSIONS

The electron spin resonance and optical absorption spectra were studied for divalent vanadium ions in NaCl. The ESR signal shows that there are two types of centers with tetragonal or orthorhombic symmetry. These centers are fairly stable and probably are V^{2+} ions associated with positive ion vacancies.

The three weak-optical absorption bands between Stark levels are located at 8190, 12 800 and 20 250 cm^{-1} which are assigned to transitions from the ground state 4A_2 to 4T_2 , ${}^4T_1(a)$, and ${}^4T_1(b)$, respectively. They yield a crystalline field strength $\Delta=8190 \text{ cm}^{-1}$ and a Racah parameter $B=559 \text{ cm}^{-1}$. One strong electron

transfer band is also found at 42 300 cm^{-1} . 4T_2 and ${}^4T_1(a)$ states have some structure, probably due to splitting by a low symmetry field while no structure is found in the ${}^4T_1(b)$ state.

The g shift and zero-field splitting may be explained by assuming that the d orbitals are considerably distorted by covalency which causes the ground state $\pm(3/2)$ level to lie below the $\pm(1/2)$ level.

ACKNOWLEDGMENTS

The author is very grateful to Dr. J. Gabriel who kindly supplied the programs for numerical computation and also wishes to express sincere thanks to Dr. P. Yuster, Dr. C. Delbecq, and Dr. S. Sugano for their encouragement and discussions and to E. Hutchinson for preparing the crystals.

Thermopowers and Resistivities of Silver-Palladium and Copper-Nickel Alloys*

P. A. SCHROEDER, R. WOLF, AND J. A. WOOLLAM

Department of Physics and Astronomy, Michigan State University, East Lansing, Michigan

(Received 28 October 1964)

The absolute thermopowers and electrical resistivities of Ag-Pd and Cu-Ni have been measured as a function of temperature between 4.2 and 300°K for concentrations up to 20 at. %. The two systems behave differently in many respects. Matthiessen's rule is obeyed well for Ag-Pd but very poorly for Cu-Ni alloys. The phonon-drag peak is completely suppressed by the addition of less than 1 at. % Ni to Cu but persists to greater than 6 at. % Pd in Ag. Nordheim-Gorter plots are curved for both alloys, but related plots for fixed concentrations are linear, indicating that any given concentration the thermopower can be considered as arising from two nearly independent scattering mechanisms, both of which have characteristic thermopowers proportional to temperature. The results in general are consistent with a rather rapid initial change in the Fermi surface up to about 0.5 at.% followed by a more gradual modification. No marked anomalies which might coincide with the departure of the Fermi surface from the zone boundary have been observed.

1. INTRODUCTION

IN this work we describe measurements of the thermoelectric power and the resistivity of silver-palladium and copper-nickel alloys. Other measurements have been made on these alloys at selected temperatures.¹⁻⁴ The present measurements are made as a function of temperature between 4.2 and 300°K for concentrations up to 20 at.% palladium and 17 at.% Ni. These have permitted (a) the study of both the diffusion and phonon-drag thermoelectric phenomena, which occur in the concentration region where the Fermi surface is expected to become detached from the zone boundary, (b) finding the temperature dependence of parameters occurring in the diffusion thermopower, (c) a com-

parison with the results of Henry and Schroeder⁵ for the Cu-Zn system.

The existence of a phonon-drag contribution to the thermopower of pure copper and silver has been established by Blatt and Kropschot,⁶ Pearson,⁷ Gold *et al.*,⁸ and Blatt *et al.*⁹ In these metals the phonon-drag thermopower is positive indicating that the contribution from umklapp processes predominates over the contribution from normal scattering processes below 100°K. Blatt and Kropschot⁶ have shown that the phonon-drag peak in copper disappears on the addition of 1% of elements (Cd, In, Sn, and Sb) which are considerably displaced from copper in the periodic system. It is

* Supported by the National Science Foundation.

¹ B. R. Coles, Proc. Phys. Soc. (London) **B65**, 221 (1952).

² J. C. Taylor and B. R. Coles, Phys. Rev. **102**, 27 (1956).

³ B. R. Coles and J. C. Taylor, Proc. Roy. Soc. (London) **267**, 139 (1962).

⁴ W. R. G. Kemp, P. G. Klemens, A. K. Sreedhar, and G. K. White, Proc. Roy. Soc. (London) **A233**, 480 (1956).

⁵ W. G. Henry and P. A. Schroeder, Can. J. Phys. **41**, 1076 (1963).

⁶ F. J. Blatt and R. H. Kropschott, Phys. Rev. **118**, 480 (1960).

⁷ W. B. Pearson, Phys. Rev. **119**, 549 (1960).

⁸ A. V. Gold, D. K. C. MacDonald, W. B. Pearson, and I. M. Templeton, Phil. Mag. **5**, 765 (1960).

⁹ F. J. Blatt, M. Garber, R. H. Kropschott, and B. Scott, Australian J. Phys. **13**, 223 (1960).